



HAL
open science

An analysis of aeolian dust in climate models

Amato T. Evan, Cyrille Flamant, Stephanie Fiedler, Owen Doherty

► **To cite this version:**

Amato T. Evan, Cyrille Flamant, Stephanie Fiedler, Owen Doherty. An analysis of aeolian dust in climate models. *Geophysical Research Letters*, 2014, 41 (16), pp.5996-6001. 10.1002/2014GL060545 . hal-01044371

HAL Id: hal-01044371

<https://hal.science/hal-01044371>

Submitted on 3 Aug 2020

HAL is a multi-disciplinary open access archive for the deposit and dissemination of scientific research documents, whether they are published or not. The documents may come from teaching and research institutions in France or abroad, or from public or private research centers.

L'archive ouverte pluridisciplinaire **HAL**, est destinée au dépôt et à la diffusion de documents scientifiques de niveau recherche, publiés ou non, émanant des établissements d'enseignement et de recherche français ou étrangers, des laboratoires publics ou privés.



RESEARCH LETTER

10.1002/2014GL060545

Key Points:

- CMIP5 models underestimate African dust emission and transport
- The dust size distribution is biased toward small particles in CMIP5 models
- CMIP5 models do not represent coupled processes that involve African dust

Supporting Information:

- Readme
- Text S1
- Table S1
- Figure S1
- Figure S2
- Figure S3

Correspondence to:

A. T. Evan,
aevan@ucsd.edu

Citation:

Evan, A. T., C. Flamant, S. Fiedler, and O. Doherty (2014), An analysis of aeolian dust in climate models, *Geophys. Res. Lett.*, 41, 5996–6001, doi:10.1002/2014GL060545.

Received 14 MAY 2014

Accepted 3 JUL 2014

Accepted article online 4 JUL 2014

Published online 18 AUG 2014

An analysis of aeolian dust in climate models

Amato T. Evan^{1,2}, Cyrille Flamant², Stephanie Fiedler³, and Owen Doherty¹

¹Scripps Institution of Oceanography, University of California San Diego, La Jolla, California, USA, ²Laboratoire Atmosphères, Milieux, Observations Spatiales, CNRS and Université Pierre et Marie Curie, Paris, France, ³School of Earth and Environment, University of Leeds, Leeds, UK

Abstract Aeolian dust is a key aspect of the climate system. Dust can modify the Earth's energy budget, provide long-range transport of nutrients, and influence land surface processes via erosion. Consequently, effective modeling of the climate system, particularly at regional scales, requires a reasonably accurate representation of dust emission, transport, and deposition. Here we evaluate African dust in 23 state-of-the-art global climate models used in the Fifth Assessment Report of the Intergovernmental Panel on Climate Change. We find that all models fail to reproduce basic aspects of dust emission and transport over the second half of the twentieth century. The models systematically underestimate dust emission, transport, and optical depth, and year-to-year changes in these properties bear little resemblance to observations. These findings cast doubt on the ability of these models to simulate the regional climate and the response of African dust to future climate change.

1. Introduction

The emission and transport of aeolian dust is both influenced by—and influences—the Earth's climate. Dust emission is controlled by both terrestrial processes and near-surface winds, the latter of which is also responsible for the subsequent transport [Marticorena and Bergametti, 1995; Shao *et al.*, 2011; Tegen *et al.*, 1996]. Suspended dust radiatively cools the surface and warms the atmosphere via direct and indirect effects [Evan *et al.*, 2009; Kaufman *et al.*, 2005a; Tegen *et al.*, 1996] and in turn can alter regional winds and rainfall [Evan *et al.*, 2011; Yoshioka *et al.*, 2007] and thus the dust aerosol cycle. Dust acts as an external source of nutrients to the oceans and remote terrestrial ecosystems [Das *et al.*, 2013; Okin *et al.*, 2011] and alters the global carbon cycle [Mahowald *et al.*, 2010]. Therefore, with respect to simulations of the climate with model biases in dust emission, concentration and deposition likely result in biases in simulated energy and nutrient budgets, yet the representation of dust in state-of-the-art climate models has not yet been systematically evaluated.

A major limitation in evaluating aeolian dust in climate models is the lack of high-quality and long-term measurements of dust. Satellite retrievals from which a dust concentration can be derived extend back to approximately 1980, but these data have uncertainties [Engelstaedter and Washington, 2007; Evan and Mukhopadhyay, 2010]. Surface measurements of visibility can go back even further, but these are not purely indicative of dust aerosol nor are they always homogeneous in time [Mahowald *et al.*, 2007]. High temporal resolution proxy records of atmospheric dust are also a source of estimates of historical concentrations, but to date these data are few [Evan and Mukhopadhyay, 2010]. Despite these shortcomings of existing mineral aerosol observations, there are a few robust data sets against which models can be evaluated. Among these we focus on observations indicating dust emission and transport from northern Africa, the world's largest dust source [Washington *et al.*, 2003]. We first examine the long-term mean dust aerosol concentration over an oceanic region west of northern Africa, 10°–20°N and 20°–30°W (Figure S1 in the supporting information). We specify this region since it includes the island nation of Cape Verde for which a long proxy record of dust exists [Evan and Mukhopadhyay, 2010], although expanding this region eastward or northward has no substantive effect on the results presented here.

2. Comparison of Dust Concentration

We first compare distributions of the annual mean dust mass path (DMP; g m^{-2}), which is the vertically integrated mass of atmospheric dust per unit area, from the Fifth Assessment Report of the Intergovernmental Panel on Climate Change (CMIP5) models (Table S1) against satellite retrievals of DMP

Table 1. Satellite and Model Long-Term Mean Optical Depth Statistics^a

	τ	τ_d	Size Bias (%)	Low Flux Bias (%)	DMP/ τ_d
AVHRR	0.38 ± 0.06	0.29 ± 0.04	-	-	2.7 ± 0.4
MODIS	0.38 ± 0.04	0.30 ± 0.03	-	-	2.7 ± 0.4
CSIRO-Mk3	0.40	0.33	100	0	1.3
GFDL-CM3	0.33	0.13	45	55	1.5
GFDL-ESM2G	0.32	0.22	73	27	1.6
GFDL-ESM2M	0.32	0.22	74	26	1.6
IPSL-CM5A-LR	0.30	0.17	55	45	1.4
IPSL-CM5A-MR	0.31	0.17	56	44	1.4
IPSL-CM5B-LR	0.30	0.16	54	46	1.4
MIROC-ESM-CHEM	0.48	0.35	100	0	1.3
MIROC-ESM	0.48	0.35	100	0	1.3
MRI-CGCM3	0.25	0.09	31	69	3.4
MRI-ESM1	0.26	0.10	33	67	2.7
Multimodel	0.34	0.22	66	34	1.7

^aShown in the second and third columns are the long-term mean τ and τ_d for AVHRR (1982–2005) and MODIS (2001–2012) and CMIP5 models (1982–2005) for which fine mode optical depth data were available. Here the model mean optical depths that are greater than or less than both satellite means are in italics and bold italics, respectively. The fourth and fifth columns are estimates of the percentage of the DMP biases (Figure 1a) that are due to biases in the size distributions of the emitted dust and the biases in the total flux of dust emitted from northern Africa. The last column is the observational (for AVHRR and MODIS) and model-estimated ratio of DMP to τ_d .

from the advanced very high resolution radiometer (AVHRR) [Stowe *et al.*, 1997] for 1982–2004 and the Moderate Resolution Imaging Spectroradiometer (MODIS) [Remer *et al.*, 2005] Terra instrument for 2000–2013. MODIS retrieved and CMIP5 output total aerosol optical depth and fine mode optical depth were used to estimate dust optical depth (τ_d) via Kaufman *et al.* [2005b], and AVHRR retrievals of total aerosol optical depth were converted to τ_d via Evan and Mukhopadhyay [2010]. We note that for the CMIP5 models the fine mode fractions for anthropogenic, mineral, and marine aerosols were nearly identical to the values reported in Kaufman *et al.* [2005b]. We conservatively estimated the uncertainty in the satellite retrievals of aerosol optical depth to be 10% for MODIS [Remer *et al.*, 2005; Shi *et al.*, 2011] and 15% for the AVHRR [Zhao *et al.*, 2008]. For the satellites, τ_d data were converted to DMP via the ratio of $2.7 \pm 0.4 \text{ g m}^{-2}$ per unit τ_d (Table 1), which is based on the average of observations of this ratio [Kaufman *et al.*, 2005b]. DMP is obtained directly from the ensemble means of the CMIP5 twentieth century historical simulations (Table S1). Two models (CCSM and CESM) only report τ_d and not DMP; therefore, we calculated the ratio of τ_d to DMP for this model using the CESM total aerosol mass fields in an overwater area where the aerosol loading is dominated by dust (2.2 g m^{-2} per unit τ_d ; Table 1). However, the inclusion of marine aerosols in the total aerosol mass field means that the τ_d to DMP ratio of 2.2 is an upper bound on the actual ratio for the model and that the DMP estimates used here for CCSM and CESM are likely too high.

For the CMIP5 data, the multimodel median DMP is 0.26 g m^{-2} , with individual model medians spanning 0.05 to 0.46 g m^{-2} (Figure 1a). In contrast, the median DMPs from the AVHRR and MODIS retrievals is 0.75 and 0.82 g m^{-2} , respectively, which is a factor of 3 larger than the multimodel median. Based on the uncertainty in the optical depth retrievals and in the τ_d to DMP ratio, the uncertainty range on the satellite-retrieved DMP is approximately 0.6 to 1.0 g m^{-2} (Figure 1a, pink shading). Compared against individual models the median satellite-retrieved DMP is larger by a factor of 2 (CCSM) to 12 (MIROC4h), and all models have a long-term median DMP that is smaller than the lower bound on the satellite-based DMP of 0.6 g m^{-2} . Furthermore, most CMIP5 models underestimate the width of the interquartile range, which is not surprising given the low bias in the mean state. We note that some models exhibit a very small range in DMP (e.g., the IPSL models), and we speculate that this is because there is no year-to-year change in the modeled dust emission, and so changes in DMP are due to variations in advection and deposition only. However, we cannot verify this because emission data for these models were not available.

3. Analysis of Dust Emission

To elucidate the source of the low bias in modeled dust mass path we calculated the long-term mean total dust emission (Tg) from northern Africa (all of Africa north of the equator) (Figure 1b), for the models for

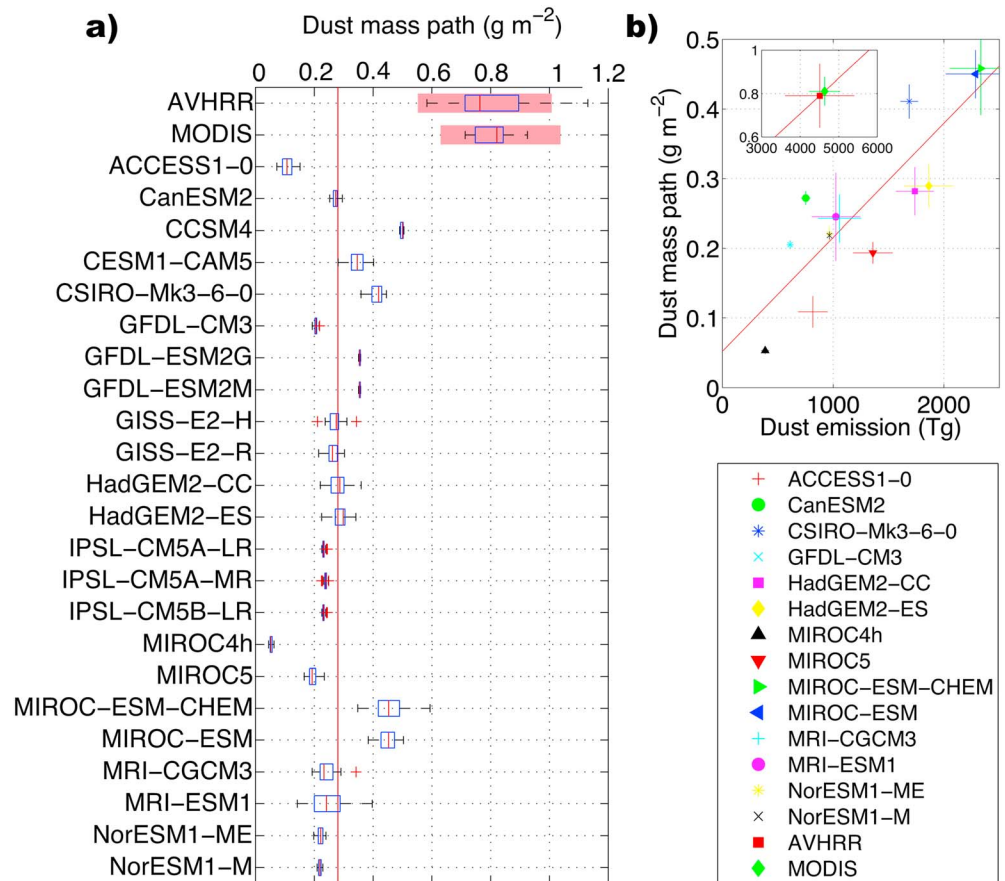


Figure 1. (a) Long-term mean dust emission and mass path from satellite retrievals and CMIP5 models. Shown in Figure 1a are box-and-whisker plots of the long-term annual mean dust mass path over the region 10°–20°N and 20°–30°W. Medians (red lines), interquartile range (blue boxes), the interquartile value ± 1.25 times the interquartile range (black “whiskers”), and outliers (red crosses) are calculated from annual mean dust mass path values over the period 1982–2004 (2000–2013 for the MODIS-Terra data). The multimodel median mass path is indicated by the red line. The red shaded regions indicate the uncertainty in the satellite estimates of long-term median DMP. (b) A scatterplot of annual mean DMP averaged over 10°–20°N and 20°–30°W (ordinate) and mean annual total dust emission from northern Africa (abscissa), for CMIP5 models (main plot) and the AVHRR and MODIS (inset), where error bars indicate the $\pm 1\sigma$ range of these data. The linear regression of DMP onto emission is indicated by the red line, which is used to estimate the satellite-based emission values.

which emission data are available (Table S1). CMIP5 models’ tropical North Atlantic DMP is directly proportional to the total northern African emission, the correlation coefficient of DMP and emission is 0.86 (p value < 0.01), and the slope of the linear regression is $1.64 \pm 0.85 \times 10^{-5} \text{ g m}^{-2} \text{ Tg}^{-1}$ (Figure 1b, red line), where the uncertainty represents the 95% confidence interval on the regression coefficient. Given the tight fit between emission and concentration, it is likely that the biases in Figure 1a are the result of dust emission biases and less to modeled transport and deposition, although they may also be related to model differences in transport related to different parameterizations of the dust size distributions or the representation of the dust size distributions in the atmosphere [Zhao *et al.*, 2013]. If we estimate the total emission from northern Africa based on the linear fit between models’ emission and mass path, but using the average mass path values from the satellites (Figure 1a), northern African dust emission is approximately $4500 \pm 1500 \text{ Tg yr}^{-1}$ (Figure 1b, inset), a factor of 3 greater than the multimodel mean emission from CMIP5 (Figure 1a).

As observations of total northern African emission do not exist there is no way to evaluate the accuracy of these model- or satellite-based estimates. Thus, while the range of model values seen here is consistent with other analysis of model output [Engelstaedter *et al.*, 2006; Huneus *et al.*, 2011], there is no a priori reason to reject the satellite estimates as being biased high. Kok [2011] found that the size distribution of dust at

emission was biased toward small particles causing larger optical depth per unit mass (τ) and speculated that the resulting dust mass emitted is underestimated by a factor of 2 to 8. This may be an artifact of tuning the models to τ observations, and we find a very good agreement in the mean τ between the model ensemble of 0.34 and the satellite-retrieved 0.38 ± 0.05 (Table 1).

However, τ is the sum of the contributions from different aerosol species, broadly categorized as marine (τ_{ma}), anthropogenic (τ_{an}), and dust (τ_d). MODIS retrievals of fine mode τ [Remer *et al.*, 2005], nominally $PM_{1.0}$, enable the separation of the MODIS [Kaufman *et al.*, 2005b] and AVHRR [Evan and Mukhopadhyay, 2010] τ into these three components. Several of the CMIP5 models also output fine mode τ (Table S1), which is also defined as $PM_{1.0}$, and thus, we are able to use the same methodology in Kaufman *et al.* [2005b] to separate the models' τ into these components (see supporting information). The comparison of modeled and satellite-retrieved τ_d shows less agreement than that for τ ; the mean satellite-retrieved τ_d is 0.30 ± 0.04 , and the multimodel mean τ_d is 0.22 (Table 1). Eight CMIP5 models have a lower τ_d (minimum of 0.09) than the satellites, two models have a higher τ_d (0.35), and one model has a mean τ_d that is within the MODIS and AVHRR uncertainty range.

For the three models in which τ_d is greater or equal to the satellite-retrieved τ_d (both MIROC models and the CSIRO-Mk3), the total DMP bias (Figure 1a) can be attributed to the size distribution of the emitted dust being too skewed toward small particles, as proposed in Kok [2011]. For the majority of models that have a mean τ_d that is smaller than the satellite-retrieved τ_d , the DMP bias can be attributed to both the dust size distribution bias and an underestimation of the total amount of dust emitted from northern Africa. In other words, a model can have a perfect representation of the dust size distribution and still underestimate the total mass flux because either the frequency of dust storms is too small or the mass flux per dust emission event is too small.

We estimate that the percentage of the low bias in DMP that is due to the skewed size distribution is $100\% \times \min\{1, \tau_{d,MODEL} / \tau_{d,MODIS}\}$ and that the percentage of the low bias in DMP that is due to an insufficient total flux is 100% minus this value. From these calculations, and averaged across all models, 66% of the bias in DMP (Figure 1a) is due to a bias in the emitted size distribution ("Size bias" in Table 1), and 34% of the bias in DMP is due to an underestimation of total northern African emission ("Flux bias" in Table 1).

The low biases in emission (Figure 1b) likely result from a number of factors, ranging from soil moisture content to vegetation cover to near-surface wind speed distributions. In an attempt to elucidate the causes of the model biases in emission and thus DMP we examined the spatial structure of surface emission across northern Africa in comparison to a satellite-derived map of emission frequency (Figures S1 and S2). Although the analysis did not provide any obvious clues for the causes of the biases, the level of disagreement between the models, between the models and observations, was stark, suggesting that the biases in emission likely result for a variety of reasons that are not necessarily consistent among the models.

4. Interannual Variability

We also examined the time evolution of DMP from CMIP5 models to evaluate the interannual variability. Here we use a hybrid satellite paleorecord of annual mean τ_d corresponding to a location adjacent to the Cape Verde islands (15°N and 23°W , Figure S1) that spans 1955–2009 (Figure 2a) and compute mass path in a manner identical to that for the AVHRR data in Figure 1a [Evan and Mukhopadhyay, 2010]. One major feature of the observational time series is the increase of τ_d over the tropical North Atlantic from the 1950s through the early 1980s and then a subsequent decline of emission and τ_d through the 2000s (Figure 2a), which is documented in satellite and in situ data sets [Evan and Mukhopadhyay, 2010; Foltz and McPhaden, 2008; Mahowald *et al.*, 2010; Prospero and Lamb, 2003]. Although the cause of these trends is still debatable, a number of papers have shown that they are either directly or indirectly caused by the simultaneous changes in summertime Sahelian rainfall, and in particular the severe drought of the 1980s [Mahowald *et al.*, 2010; Prospero and Lamb, 2003; Cowie *et al.*, 2013], although new work has shown these trends to be only the result of a "slowdown" of the surface winds over the Sahara [Ridley *et al.*, 2014].

We regressed a time series of observed June–September averaged Sahelian rainfall rates onto the proxy record of DMP to quantify this dependency for 1960–2004. Sahel precipitation data from the Joint Institute for the Study of the Atmosphere and Ocean (doi: 10.6069/H5MW2F2Q), which uses Sahel averaging regions from Janowiak [1988]. The observed coefficient of the regression is $-0.06 \pm 0.04 \text{ g m}^{-2} \text{ mm}^{-1} \text{ d}^{-1}$, which is

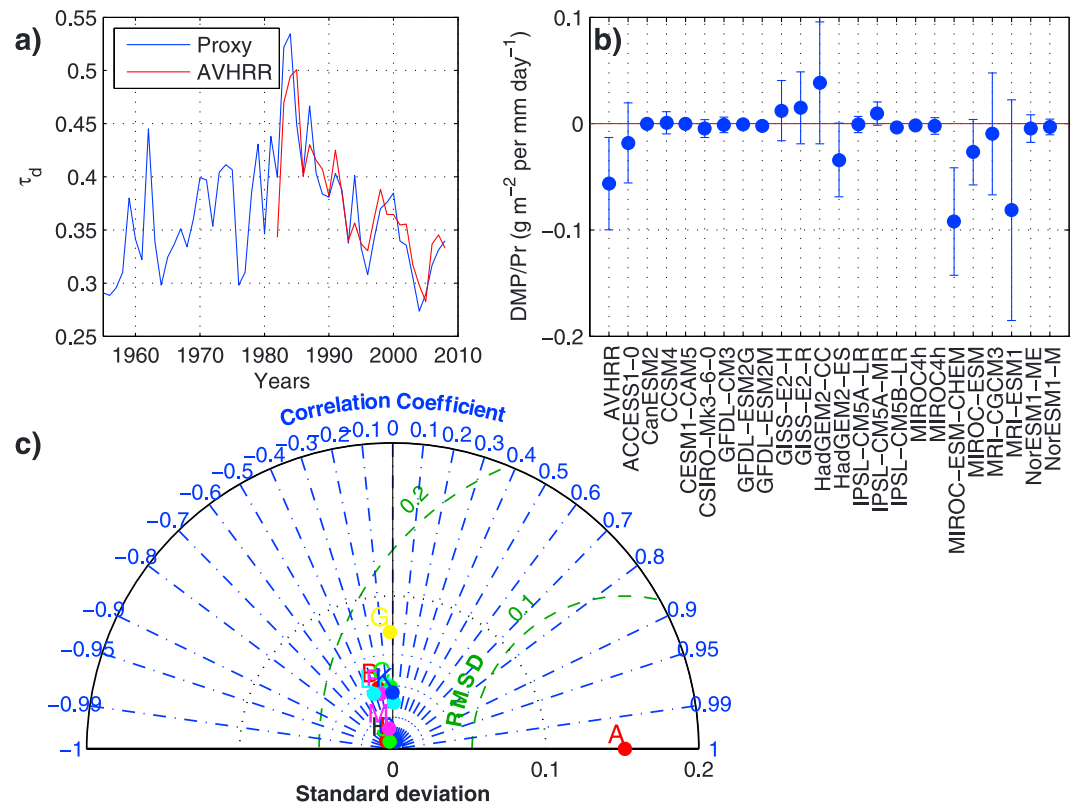


Figure 2. Annual variability of modeled and observed dust. (a) Plotted are the proxy and AVHRR annual mean time series of τ_d averaged over 10° – 20° N and 20° – 30° W. (b) Plotted are the coefficients (filled circles) and their 95% certainty levels (bars) from the regression of AVHRR and modeled DMP onto observed (for the AVHRR only) and modeled June–September Sahelian rainfall (10° – 20° N and 15° W– 20° E), calculated with data from 1960 to 2004. (c) A Taylor diagram for annual mean DMP for 1960–2004 and averaged over 10° – 20° N and 20° – 30° W. The red circle marked “A” represents the proxy record of DMP shown in Figure 2c, and the other markers are CMIP5 models (see Table S1 for legend). The abscissa and dotted black semicircles represent the time series’ standard deviation, the dashed green semicircles are the root-mean-square differences between the models and the proxy record, and the radial blue dash-dotted lines are the correlation coefficients of the model time series and the proxy record.

statistically different from zero at the 95% significance level (Figure 2b). Using the models’ rainfall rates and DMP for the same years (Figure 2b), only the MIROC-ESM-CHEM has a negative regression coefficient that is statistically different from zero at the 95% level (Figure 2b). Consistent with our findings, a recent study found that a subset of the models evaluated here exhibited a negative correlation between DMP over the tropical North Atlantic and the phase of the modeled Atlantic Multidecadal Oscillation in twentieth century historical forcing runs, although the change was not determined to be statistically significant [Martin et al., 2014].

We also compared annual mean DMP from AVHRR retrievals to model output for the CMIP5 Atmospheric Model Intercomparison Project simulations for the years 1982–2006. From a Taylor diagram [Taylor, 2001], none of the models (B–L in Figure 2c) exhibit a statistically significant and positive correlation to the data (A in Figure 2c), where the multimodel mean and median correlation coefficients are both less than zero. Also, the root-mean-squared biases are similar in magnitude to the observational data’s standard deviation, indicating a complete lack of correspondence between the model output and satellite retrievals. Similar results are found when comparing the proxy DMP data [Evan and Mukhopadhyay, 2010] and the model output from the historical forcing runs for 1960–2004 (Figure S2).

5. Conclusions

Based on the results presented here CMIP5 models are unable to capture any of the salient features of northern African dust emission and transport. The exact nature of the biases are not elucidated here but are likely to be related to a variety of sources, including the dust size distributions and atmospheric and surface

processes. We conclude that there is no reason to assume that the projections of dust emission and concentration for the 21st century have any validity. Despite highlighting deficiencies in the representation of the multitude of land and atmospheric processes that govern dust emission, these results also cast doubt on the representation of other features of coupled Earth system that are affected by aeolian dust, including regional land and ocean surface temperatures [Evan *et al.*, 2009], precipitation and cloud processes [Kaufman *et al.*, 2005a; Yoshioka *et al.*, 2007], coupled equatorial processes [Evan *et al.*, 2011], and terrestrial [Das *et al.*, 2013] and oceanic biogeochemistry [Mahowald *et al.*, 2010]. It is likely that the representation of dust in climate models can be improved by increasing the number and quality of observations of dust emission and atmospheric mass concentration in order to improve understanding of the processes affecting dust emission.

Acknowledgments

We acknowledge Ian Eisenman, Kerstin Schepanski, and two anonymous reviewers for comments on the methodologies and the satellite emission map used in this study. This work was supported by the French Agence Nationale de la Recherche (ANR) grant ANR-10-LABX-18-01 of the national Programme Investissements d'Avenir. Funding for this work was also provided by Laboratoire d'excellence Institute Pierre Simon Laplace (L-IPSL), a grant from the "Research in Paris" program, and National Oceanographic and Atmospheric Administration Climate Program Office grant NA11OAR4310157. AVHRR data from the National Oceanic and Atmospheric Administration National Climatic Data Center at <http://www.ncdc.noaa.gov/cdr/operationalcds.html>. MODIS data from the Giovanni online data system, developed and maintained by the NASA GES DISC at <http://disc.sci.gsfc.nasa.gov/giovanni>.

The Editor thanks two anonymous reviewers for their assistance in evaluating this paper.

References

- Cowie, S. M., P. Knippertz, and J. H. Marsham (2013), Are vegetation-related roughness changes the cause of the recent decrease in dust emission from the Sahel?, *Geophys. Res. Lett.*, *40*, 1868–1872, doi:10.1002/grl.50273.
- Das, R., A. T. Evan, and D. Lawrence (2013), Contributions of long-distance dust transport to atmospheric P inputs in the Yucatan Peninsula, *Global Biogeochem. Cycles*, *27*, 167–175, doi:10.1029/2012GB004420.
- Engelstaedter, S., and R. Washington (2007), Atmospheric controls on the annual cycle of North African dust, *J. Geophys. Res.*, *112*, D03103, doi:10.1029/2006JD007195.
- Engelstaedter, S., I. Tegen, and R. Washington (2006), North African dust emissions and transport, *Earth Sci. Rev.*, *79*(1–2), 73–100.
- Evan, A. T., and S. Mukhopadhyay (2010), African dust over the northern tropical Atlantic: 1955–2008, *J. Appl. Meteorol. Climatol.*, *49*, 2213–2229.
- Evan, A. T., D. J. Vimont, R. Bennartz, J. P. Kossin, and A. K. Heidinger (2009), The role of aerosols in the evolution of tropical North Atlantic Ocean temperature, *Science*, *324*(5928), 778–781.
- Evan, A. T., G. R. Foltz, D. Zhang, and D. J. Vimont (2011), Influence of African dust on ocean–atmosphere variability in the tropical Atlantic, *Nat. Geosci.*, *4*, 762–765, doi:10.1038/ngeo1276.
- Foltz, G. R., and M. J. McPhaden (2008), Trends in Saharan dust and tropical Atlantic climate during 1980–2006, *Geophys. Res. Lett.*, *35*, L20706, doi:10.1029/2008GL035042.
- Huneus, N., et al. (2011), Global dust model intercomparison in AeroCom phase I, *Atmos. Chem. Phys.*, *11*, 7781–7816, doi:10.5194/acp-11-7781-2011.
- Janowiak, J. E. (1988), An investigation of interannual rainfall variability in Africa, *J. Clim.*, *1*, 240–255.
- Kaufman, Y. J., I. Koren, L. A. Remer, D. Rosenfeld, and Y. Rudich (2005a), The effect of smoke, dust, and pollution aerosol on shallow cloud development over the Atlantic Ocean, *Proc. Natl. Acad. Sci. U.S.A.*, *102*, 11,207–11,212.
- Kaufman, Y. J., I. Koren, L. A. Remer, D. Tarré, P. Ginoux, and S. Fan (2005b), Dust transport and deposition observed from the Terra-Moderate Resolution Imaging Spectroradiometer (MODIS) spacecraft over the Atlantic Ocean, *J. Geophys. Res.*, *110*, D10S12, doi:10.1029/2003JD004436.
- Kok, J. F. (2011), A scaling theory for the size distribution of emitted dust aerosols suggests climate models underestimate the size of the global dust cycle, *Proc. Natl. Acad. Sci. U.S.A.*, *108*, 1016–1021.
- Mahowald, N. M., J. A. Ballantine, J. Feddema, and N. Ramankutty (2007), Global trends in visibility: Implications for dust sources, *Atmos. Chem. Phys.*, *7*, 3309–3339, doi:10.5194/acp-7-3309-2007.
- Mahowald, N. M., et al. (2010), Observed 20th century desert dust variability: Impact on climate and biogeochemistry, *Atmos. Chem. Phys.*, *10*, 10,875–10,893, doi:10.5194/acp-10-10875-2010.
- Marticorena, B., and G. Bergametti (1995), Modeling the atmospheric dust cycle: 1. Design of a soil-derived dust emission scheme, *J. Geophys. Res.*, *100*(D8), 16,415–16,430, doi:10.1029/95JD00690.
- Martin, E. R., C. Thorncroft, and B. B. Booth (2014), The multidecadal Atlantic SST—Sahel rainfall teleconnection in CMIP5 simulations, *J. Clim.*, *27*, 784–806.
- Okin, G. S., et al. (2011), Impacts of atmospheric nutrient deposition on marine productivity: Roles of nitrogen, phosphorus, and iron, *Global Biogeochem. Cycles*, *25*, GB2022, doi:10.1029/2010GB003858.
- Prospero, J. M., and P. J. Lamb (2003), African droughts and dust transport to the Caribbean: Climate change implications, *Science*, *302*(5647), 1024–1027.
- Remer, L. A., et al. (2005), The MODIS aerosol algorithm, products, and validation, *J. Atmos. Sci.*, *62*, 947–973.
- Ridley, D. A., C. L. Heald, and J. M. Prospero (2014), What controls the recent changes in African mineral dust aerosol across the Atlantic?, *Atmos. Chem. Phys. Discuss.*, *14*, 3583–3627, doi:10.5194/acpd-14-3583-2014.
- Shao, Y., et al. (2011), Dust cycle: An emerging core theme in Earth system science, *Aeolian Res.*, *2*(4), 181–204.
- Shi, Y., J. Zhang, J. S. Reid, B. Holben, E. J. Hyer, and C. Curtis (2011), An analysis of the collection 5 MODIS over-ocean aerosol optical depth product for its implication in aerosol assimilation, *Atmos. Chem. Phys.*, *11*, 557–565, doi:10.5194/acp-11-557-2011.
- Stowe, L. L., A. M. Ignatov, and R. R. Singh (1997), Development, validation, and potential enhancements to the second generation operational aerosol product at the National Environmental Satellite, Data, and Information Service of the National Oceanic and Atmospheric Administration, *J. Geophys. Res.*, *102*(D14), 16 923–16 934, doi:10.1029/96JD02132.
- Taylor, K. E. (2001), Summarizing multiple aspects of model performance in a single diagram, *J. Geophys. Res.*, *106*(D7), 7183–7192, doi:10.1029/2000JD900719.
- Tegen, I., A. A. Lacis, and I. Y. Fung (1996), The influence of mineral aerosol from disturbed soils on the global radiation budget, *Nature*, *380*, 419–422.
- Washington, R., M. Todd, N. J. Middleton, and A. S. Goudie (2003), Dust-storm source areas determined by the total ozone monitoring spectrometer and surface observations, *Ann. Assoc. Am. Geogr.*, *93*, 297–313, doi:10.1111/1467-8306.9302003.
- Yoshioka, M., N. M. Mahowald, A. J. Conley, W. D. Collins, D. W. Fillmore, C. S. Zender, and D. B. Coleman (2007), Impact of desert dust radiative forcing on Sahel precipitation: Relative importance of dust compared to sea surface temperature variations, vegetation changes, and greenhouse gas warming, *J. Clim.*, *20*, 1445–1467.
- Zhao, C., S. Chen, L. R. Leung, Y. Qian, J. F. Kok, R. A. Zaveri, and J. Huang (2013), Uncertainty in modeling dust mass balance and radiative forcing from size parameterization, *Atmos. Chem. Phys.*, *13*, 10,733–10,753, doi:10.5194/acp-13-10733-2013.
- Zhao, T. X.-P., I. Laszlo, W. Guo, A. Heidinger, C. Cao, A. Jelenak, D. Tarpley, and J. Sullivan (2008), Study of long-term trend in aerosol optical thickness observed from operational AVHRR satellite instrument, *J. Geophys. Res.*, *113*, D07201, doi:10.1029/2007JD009061.